

Temperature-Profile Methods for Estimating Percolation Rates in Arid Environments

Jim Constantz,* Scott W. Tyler, and Edward Kwicklis

ABSTRACT

Percolation rates are estimated using vertical temperature profiles from sequentially deeper vadose environments, progressing from sediments beneath stream channels, to expansive basin-fill materials, and finally to deep fractured bedrock underlying mountainous terrain. Beneath stream channels, vertical temperature profiles vary over time in response to downward heat transport, which is generally controlled by conductive heat transport during dry periods, or by advective transport during channel infiltration. During periods of stream-channel infiltration, two relatively simple approaches are possible: a heat-pulse technique, or a heat and liquid-water transport simulation code. Focused percolation rates beneath stream channels are examined for perennial, seasonal, and ephemeral channels in central New Mexico, with estimated percolation rates ranging from 100 to 2100 mm d⁻¹. Deep within basin-fill and underlying mountainous terrain, vertical temperature gradients are dominated by the local geothermal gradient, which creates a profile with decreasing temperatures toward the surface. If simplifying assumptions are employed regarding stratigraphy and vapor fluxes, an analytical solution to the heat transport problem can be used to generate temperature profiles at specified percolation rates for comparison to the observed geothermal gradient. Comparisons to an observed temperature profile in the basin-fill sediments beneath Frenchman Flat, Nevada, yielded water fluxes near zero, with absolute values <10 mm yr⁻¹. For the deep vadose environment beneath Yucca Mountain, Nevada, the complexities of stratigraphy and vapor movement are incorporated into a more elaborate heat and water transport model to compare simulated and observed temperature profiles for a pair of deep boreholes. Best matches resulted in a percolation rate near zero for one borehole and 11 mm yr⁻¹ for the second borehole.

BY THE EARLY 1900s, researchers intuitively understood that heat is transferred during the course of water movement through porous material, and that temperature profiles within the material are strongly influenced by water movement (Bouyoucos, 1915). As a consequence, temperature profiles above the water table might provide a basis for quantifying water fluxes. Challenges in collecting temperature profiles and the resources necessary to quantitatively solve complex heat and water transport models limited the utility of analyzing temperature patterns in the vadose zone. Recently both the measurement of temperature and the simulation of heat and water transport have benefited from significant advances in temperature acquisition and computer resources. These advances facilitate the measurement and analysis of temperature in the vadose zone, such that the link between temperature and water fluxes that was appreciated in the early 1900s is now being quantified in environments ranging from soils (e.g., Taniguchi and Sharma, 1993; Tabbagh et al., 1999)

to sediments beneath stream channels to (e.g., Constantz et al., 1994; Izbicki and Michel, 2002) to deep basin-scale flow systems (e.g., Reiter, 2001).

Here we describe the general trends in temperature patterns common in the vadose zone of arid environments and the manner in which these patterns may be analyzed to estimate percolation rates. Temperature profiles for three common topographies in arid regions are examined to delineate several approaches for estimating vertical water fluxes at various depths, and to provide insight into the variability of percolation patterns with depth in arid regions. The first case examines the potential for determining focused percolation beneath stream channels, the second examines the potential for determining diffuse percolation within vast inter-channel basin-fill material, and the third case examines the potential for determining deep percolation within fractured bedrock underlying mountainous terrain.

Temperature Profiles in the Vadose Zone of Arid Environments

On an annual time scale, temperature patterns in the shallow vadose zone are distinctly different from those in the deep vadose zone. Temperatures in the shallow vadose zone vary both with depth and time, while temperatures in the deeper vadose zone vary only with depth (i.e., show temporal stability). Below the depth of seasonal temperature variability, a region of uniformly increasing temperature with depth exists due to upward conduction of heat from the earth's warmer interior, termed the *geothermal heat flux*. There is a large spatial variation in the magnitude of this heat flux, primarily due to spatial variations in crustal heating and proximity to magmatic activity (Lachenbruch and Sass, 1977), as well as spatial variations in groundwater fluxes (Bredenhoeft and Papadopoulos, 1965). The resulting rate of temperature change with depth is commonly referred to as the *geothermal gradient*. If thermal conduction is the sole transport mechanism, the thermal conductivity of the solid, liquid, and gas phases, and the underlying geothermal heat flux determine the magnitude of the geothermal gradient for a given location. Processes such as percolation generally serve to alter the temperature gradient. (Note that *infiltration* is the flux of water into the vadose zone, *percolation* is the flux of water through the vadose zone, *recharge* is the flux of water into the underlying water table, and *discharge* is the upward flux of water from the water table.) Figure 1 (upper) depicts hypothetical temperature profiles between the surface and a depth of 200 m, for the case of groundwater discharge, no flux, and groundwater recharge. A distinct lineation is depicted between a shallow region of varying temperature profiles during the course of the year and a deeper region of time invariant temperature profiles during the year. In Fig. 1 (upper), the seasonal tempera-

J. Constantz, U.S. Geological Survey, Menlo Park, CA 94025; S.W. Tyler, University of Nevada, Reno, NV 89557; E. Kwicklis, Los Alamos National Laboratory, Los Alamos, NM, 87545. Received 13 Mar. 2002. Reviews and Analyses. V02-0015. *Corresponding author (jconstan@usgs.gov).

ture extinction depth resides at approximately 30 m, below which no seasonal variation in temperature is observed. Within in the shallow region, the yearly temperature envelope encompasses the annual range of temperature at each depth above 30 m. Figure 1 (lower panel) depicts temperature profiles between the surface and a depth of 2 m, for winter vs. summer conditions, in the presence or absence of percolation. This creates daily temperature envelopes for each of the four separate conditions. For this hypothetical case, the daily temperature extinction depth is the location below which no daily variation in temperature is detected, or approximately 0.5 m in the absence of water flux, and approximately 2 m during percolation.

As suggested by Fig. 1, the heat transport processes that occur in the vadose zone can be diverse and complex, warranting a complete physically based equation to fully describe all of the heat and water transport processes. Under sinusoidal varying surface temperature (diurnal and seasonal), temperature fluctuations in the vadose zone decline with depth. Once below the seasonal temperature extinction depth (ranging from 5 to 30 m in porous unsaturated media), thermal flux in basin-fill sediments is controlled primarily by conduction, advection (through the flux of liquid water), and diffusive transport of latent heat by water vapor. As shown by Philip and de Vries (1957), Sophocleous (1979), Scanlon and Milly (1994), and others, liquid flux driven by thermally induced changes in capillary pressure, that is, coupled liquid-thermal transport, is most important in regions of large thermal gradient, in the range of $10^{\circ}\text{C m}^{-1}$. This temperature range often occurs at the ground surface and diminishes rapidly with depth in the vadose zone toward the geothermal gradient, which is in the range of $0.01^{\circ}\text{C m}^{-1}$. Mineral weathering and clay hydration represent another potential source-sink of thermal energy; however, this contribution to the total heat flux is likely to be restricted to unique geologic environments. In unsaturated fractured porous media, advection of sensible and latent heat in the gas phase may also be significant, but is likely to be much smaller in most unsaturated, porous media where air permeabilities are smaller.

The work of Philip and de Vries (1957) continues to stand today as the seminal work on water (both liquid and vapor) transport under temperature gradients encountered in the shallow vadose zone. Sophocleous (1979) developed coupled fluid and heat transport solutions for the vadose zone, demonstrating that inclusion of the coupling of the transport equations is necessary where thermal gradients are large and water fluxes significant. Scanlon (1994) and Scanlon and Milly (1994) simulated thermally driven water and vapor transport in shallow (15 m) vadose zone profiles in west Texas, demonstrating that vapor transport driven by seasonal temperature fluctuations is a significant transport mechanism in arid vadose zones. For temperature gradients encountered at greater depths, Sass et al. (1988) suggested that very small amounts of percolation could be responsible for large areas of anomalously low crustal heat flux in portions of the Great Basin of the western

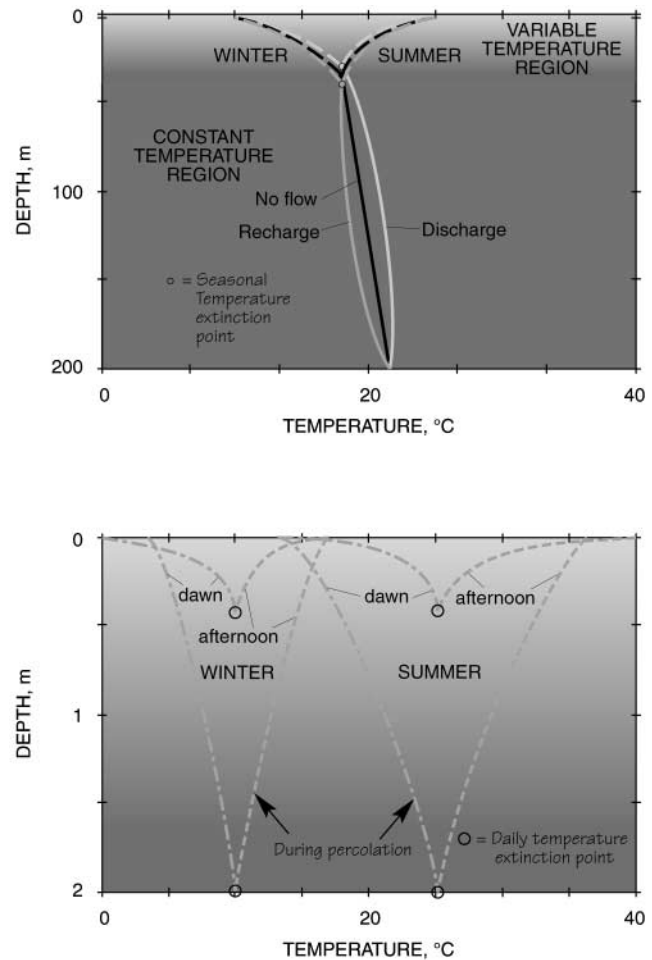


Fig. 1. Hypothetical deep and shallow temperature profiles for the region of variable temperature and the region of constant temperature with time (i.e., region of temporal stability).

United States. Walvoord et al. (1999) suggested that upward vapor transport encountered at some locations in deep vadose zones may be responsible for the observations of nearly uniform capillary pressures with depth at these locations. Consequently, a comprehensive quantitative description of transient, multiphase flow in these types of arid environments requires a detailed knowledge of the thermal properties in the domain of interest, accurate definition of boundary and initial conditions, and detailed characterization of stratigraphy to fully describe heat and water transport in the liquid and vapor phases.

These stringent requirements have prompted alternative approaches, using simplifying assumptions, to develop a more tractable problem. We review several approaches as potential techniques for analysis of temperature profiles derived from a range of locations and depths in the vadose zone of the U.S. Southwest.

ANALYSIS OF SHALLOW TEMPERATURE PROFILES BENEATH STREAM CHANNELS IN ARID REGIONS

In the presence of streamflow, water and heat transport in the vapor phase can be assumed negligible within

the underlying streambed, condensing the multiphase problem to a more computationally manageable expression. Suzuki (1960) and Stallman (1963, 1965) independently developed an expression for saturated vertical flow in the z -direction as follows:

$$K_T \frac{\partial^2 T}{\partial z^2} - q_l C_w \frac{\partial T}{\partial z} = C_s \frac{\partial T}{\partial t}, \quad [1]$$

where K_T is thermal conductivity ($\text{J s}^{-1} \text{m}^{-1} \text{°C}^{-1}$), T is temperature (°C), z is elevation with z positive upwards (m), q_l is liquid flux (m s^{-1}), C_w and C_s are the volumetric heat capacities of water and the bulk sediment ($\text{J m}^{-3} \text{°C}^{-1}$), and t is time (s). The value of q_l is defined by Darcy's equation as a product of the hydraulic conductivity, K (m s^{-1}), and the total head gradient, h . Equation [1] as written assumes that K_T is uniform with depth. If this is not the case, K_T must be inside the partial differential. When q_l is zero, the equation reduces to the Fourier equation for the transfer of heat by conduction, and when q_l is large, advection dominates the transfer of heat, as well as the change of temperature throughout the porous material. Within Eq. [1] thermal parameters can be estimated given some knowledge of porous materials. The heat capacity of the bulk sediment can be estimated by the following:

$$C_s = f_s(c_s \rho_s) + f_w(c_w \rho_w) + f_a(c_a \rho_a) \quad [2]$$

where f_s , f_w , and f_a are the volumetric fractions of the sediment, water, and air, respectively; c_s , c_w , and c_a are specific heats ($\text{J kg}^{-1} \text{°C}^{-1}$) of the sediment, water, and air, respectively; and ρ_s , ρ_w , and ρ_a are the densities (kg m^{-3}) of the sediment, water, and air, respectively. The product of the specific heat capacity and the density is the volumetric heat capacity, which is approximately 0.8×10^6 , 4.2×10^6 , and $0.001 \times 10^6 \text{ J m}^{-3} \text{°C}^{-1}$ for sediments, water, and air, respectively (de Vries, 1963). Numerous researchers have demonstrated that Eq. [1] is quite successful in estimating saturated heat and groundwater flow in both shallow (e.g., Cartwright, 1974) and deep environments (e.g., Bredehoeft and Papadopoulos, 1965).

A simplification of Eq. [1] is employed for the case where pore water velocities are sufficiently high, such that heat transport by conduction is negligible compared with heat transport by advection (e.g., Nightingale, 1975). This case is typical during flow events in many ephemeral streambeds in arid environments, especially near the mountain front. These high energy stream channels often possess highly permeable bed materials, which inhibit sustained streamflow except during atypically long events. For those cases where conduction is small compared with advection, q_l is approximated by:

$$q_l = V_T(c_s/c_w) \quad [3]$$

where V_T (m s^{-1}) is the vertical velocity or travel time of the temperature peak (i.e., temperature maximum) into the streambed sediments. This heat-pulse or thermal tracking technique has been shown to work well in a laboratory column comparison with bromide tracer (Taniguchi and Sharma, 1990), and the technique has been successfully applied beneath Tijeras Arroyo, New

Mexico (Constantz and Thomas, 1996, 1997) by monitoring temperatures to a depth of 3 m during seasonal ephemeral flows.

A more comprehensive approach is warranted to account for simultaneous conductive and advective heat transport beneath streambeds that sustain longer duration streamflows. To implement this more comprehensive approach, a heat transport equation may be developed via the convective–dispersion equation (e.g., see Kipp, 1987) as follows:

$$\frac{\partial[\theta C_w + (1 - \phi) C_s]}{\partial t} = \frac{\partial}{\partial z} \left[K_t(\theta) \frac{\partial T}{\partial z} \right] + \frac{\partial}{\partial z} \left(\theta C_w D_h \frac{\partial T}{\partial z} \right) - \frac{\partial}{\partial z} (\theta C_w T q_l) + Q C_w T \quad [4]$$

where θ is percentage volumetric water content, ϕ is sediment porosity (dimensionless), D_h is the thermomechanical dispersion tensor ($\text{m}^2 \text{s}^{-1}$), q_l is the liquid water flux (m s^{-1}), and Q is the rate of fluid source (s^{-1}). The left side of the equation represents the change in energy stored in a volume over time. The first term on the right side describes the energy transport by heat conduction through the bulk material. The second term on the right side accounts for thermomechanical dispersion. The third term on the right side represents advective heat transport, and the final term on the right side represents heat sources or sinks to mass movement into or out of the volume. To describe simultaneous water flow in the vadose zone, the variably saturated groundwater flow equation can be expressed as follows:

$$\frac{\partial \theta(z, t)}{\partial t} = \frac{\partial}{\partial z} \left[K(\psi, z) \frac{\partial h(z, t)}{\partial z} \right], \quad [5]$$

where ψ is the water pressure head (m) and h is the total head (m) (Buckingham, 1907; Richards, 1931). Within Eq. [4] the thermomechanical dispersion tensor is defined as (Healy, 1990):

$$D_h = \alpha_T |v| \delta_{ij} + \frac{(\alpha_l - \alpha_t) v_i v_j}{v}, \quad [6]$$

where α_l and α_t are longitudinal and transverse dispersivities, respectively (m); δ_{ij} is the Kronecker delta function; v_i and v_j are the i th and j th component of the velocity vector, respectively (m s^{-1}), and $|v|$ is the magnitude of the velocity vector (m s^{-1}).

Both the hydraulic conductivity, K , and the thermal conductivity, K_T , vary with texture and degree of saturation; however, the total variation in K_T is small compared with K and is more accurately predicted from texture and moisture content information (van Duin, 1963). Thus, K_T is generally estimated, and K is varied in the course of matching observed temperatures through inverse simulation modeling. The two-dimensional forms of Eq. [4] and [5] are solved numerically in the computer simulation code, VS2DH (Healy and Ronan, 1996). VS2DH was developed specifically for stream channels and is restricted to environments in which heat and water transport in the vapor phase are small relative to transport in the liquid phase. Ronan et al. (1998) successfully applied VS2DH to simulate groundwater flow

pattern below Vice Canyon, Nevada, by inversely matching simulated sediment temperatures to observed temperatures.

Using this approach for temperature-based estimates of flux beneath channels, the primary uncertainty is a result of uncertainties in the thermal parameters, K_T , C_s , and in extreme cases T . Niswonger and Rupp (2000) applied Monte Carlo analysis to VS2DH simulations for determining the relative impacts in random errors in the thermal parameters beneath streambeds. They concluded that errors in T produced significantly greater uncertainties in percolation rates compared with K_T and C_s . Generally this does not present a problem, since T is routinely measured with great accuracy. However, as advective heat transport diminishes with decreasing percolation rates, the relative importance of the K_T and C_s increases, such that their characterization is critical as q_1 approaches zero.

Results from three sites in central New Mexico are presented with a range of streamflow conditions to aid in demonstrating the various approaches necessary to derive streambed water fluxes for distinctly different streambed temperature signals.

Rio Grande, New Mexico

The Rio Grande is a wide, generally shallow (<3 m), perennial stream as it flows through central New Mexico. Traditional methods of determining seepage losses are hampered by undocumented withdrawals and return flows along virtually all reaches in the greater Albuquerque area. In this study, losses were monitored by direct estimates of streambed percolation using heat as tracer of groundwater flow. Temperatures were logged in several piezometers between the surface and depths of approximately 15 m below the streambed of the Rio Grande as described in Bartolino and Niswonger (1999). In a procedure similar to Lapham (1989), piezometers were temperature logged seven times at approximately 1-m vertical intervals from September 1996 to August 1998. Figure 2 shows the observed annual temperature envelope for a site 30 m north of the Paseo del Norte bridge. The temperature envelope in Fig. 2 possesses a tulip shape compared with the fanned out shape of the hypothetical envelope in Fig. 1. This shape suggests an abrupt decrease in the rate of heat transport below 5 m, as the slope sharply increases due to lack of transport. Also, note that the seasonal temperature extinction depth is below the depth of observation. Inverse modeling was performed using VS2DH and the parameter estimating code, PEST (Doherty et al., 1994). The stream stage and hydraulic gradient were measured along with stream and streambed temperatures; then simulated temperatures were fit to observed sediment temperatures by inverse modeling using PEST. Figure 3 gives an example of the excellent optimized fit achieved compared with observed sediment temperature at this site. The optimized fluxes yielded streambed fluxes ranging from 8 mm d⁻¹ for September 1996 to 80 mm d⁻¹ for January 1997. The higher percolation rates estimated in the win-

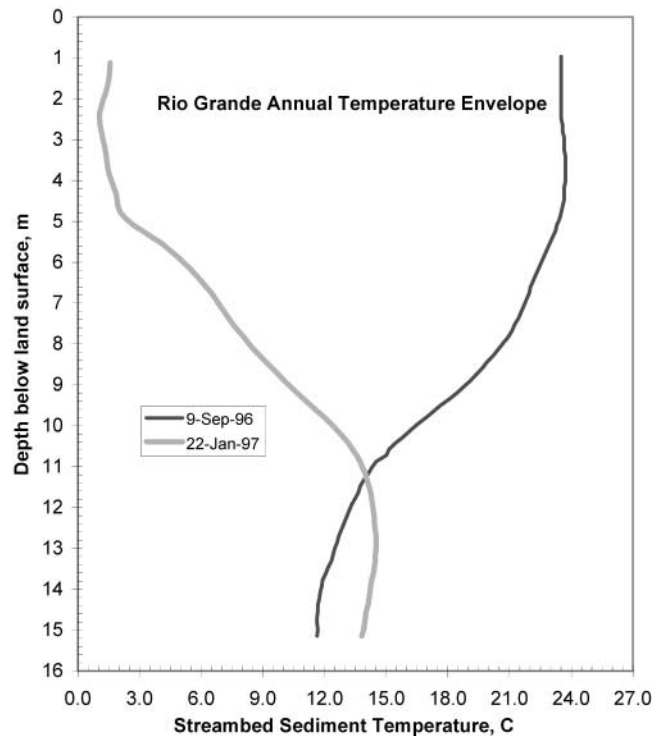


Fig. 2. Observed annual temperature envelope beneath the Rio Grande near Albuquerque, NM.

ter were possibly the result of scour removal of summer fines and/or raised winter stages.

Bear Canyon, New Mexico

Bear Canyon is located on the eastern edge of Albuquerque, NM and drains surface water from the western flanks of the Sandia Mountains into the Middle Rio Grande Basin. The stream is representative of numerous

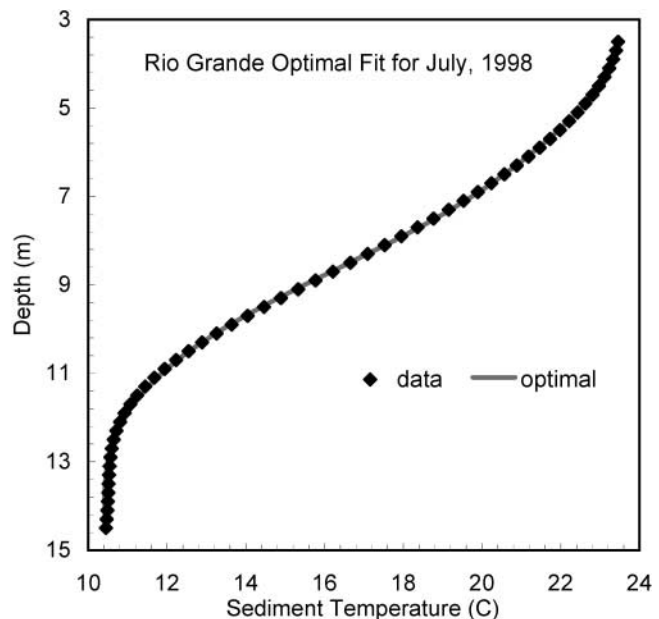


Fig. 3. Optimal simulated inverse fit compared with observed temperatures beneath the Rio Grande near Albuquerque, NM, for July 1998.

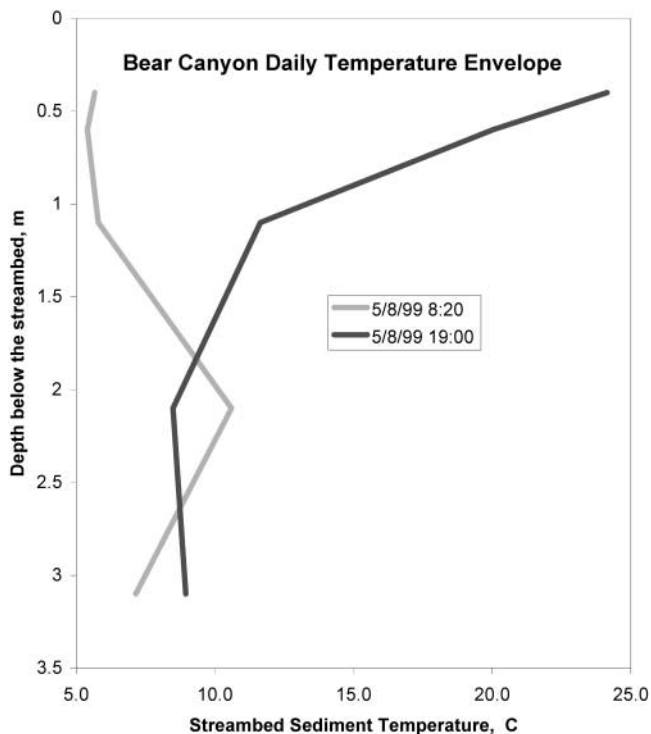


Fig. 4. A typical daily temperature envelope beneath Bear Canyon, NM.

mountain-front streams derived from the Sandia and Manzano Mountains with undetermined potential for recharging the basin at the margins. Vertical temperature patterns were monitored beneath the stream channel at several locations along Bear Canyon, west of the bedrock contact. This was accomplished using a series of thermocouple wires placed at depths between the streambed surface and about 3 m below the channel with a truck-mounted drill rig. Thermocouples were connected to a datalogger, and temperatures were logged at 15-min intervals from 1996 through 1999. Seasonal snowmelt resulted in a gradual progression of the location of the streamflow down channel for several months in the spring, followed by streamflow recession up channel in early summer. Figure 4 shows a daily temperature envelope for 8 May 1999, which is qualitatively similar to the percolation temperature envelopes depicted in Fig. 1 (lower). There is great uncertainty in capturing the exact maximum and minimum temperatures during the rapid changes near the surface because of the necessity of using a practical sample frequency of at least 15 min. This uncertainty was minimized by using time series thermographs, where interpolation leads to estimates of the daily temperature extremes. Figure 5 shows

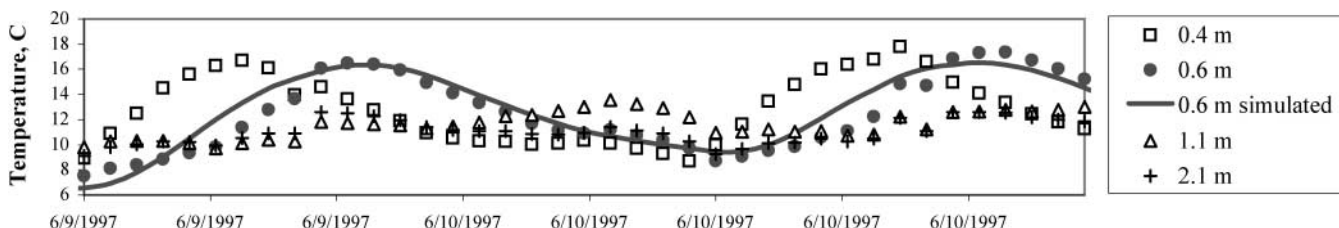


Fig. 5. The observed sediment-temperature patterns approximately 275 m west of the mountain-front in Bear Canyon, NM, compared with optimal simulated temperatures at a depth of 0.6 m during June 1997.

time series thermographs for sediment temperatures at four depths below the streambed at a channel location approximately 275 m west of the mountain front during June 1997. The figure also shows the simulated best fit at 0.60 m using VS2DH and PEST. An average vertical streambed percolation rate of 770 mm d^{-1} resulted from optimized simulations during the duration of spring streamflow for this site.

Santa Fe River, New Mexico

The Santa Fe River is a highly controlled stream that flows south from the Sangre de Cristo Range, becoming ephemeral as it passes through Santa Fe, NM. Stream loss through this reach may represent a significant component of total recharge to the underlying aquifer. Two streambed temperature procedures were examined to estimate streambed percolation rates in a study reach below a control structure with a U.S. Geological Survey streamgaging station. Temperature nests were installed between the streambed surface and about 2.0 m depth at sites along the study reach between March and June 1999. Streamflows are ephemeral in this reach of the river, often lasting only several hours, such that time series thermographs are the only option. A brief $0.67 \text{ m}^3 \text{ s}^{-1}$ streamflow event that occurred on 24 May was selected as an example for estimating streambed percolation rates at instrumented locations below the stream gage. Figure 6 depicts the best-fit match to the measured data using simulated results from VS2DH at one location in the streambed. Based on this match, initial percolation rates beneath the channel were estimated as $2.5 \times 10^{-5} \text{ m s}^{-1}$, and then rapidly dropped to $1.2 \times 10^{-6} \text{ m s}^{-1}$.

As a second temperature procedure, the temperature arrival-time method expressed in Eq. [3] was used to estimate initial percolation rates beneath the channel. The initial rate between the surface and a depth of 0.068 m was calculated as $2.18 \times 10^{-5} \text{ m s}^{-1}$, but the brief nature of the event prevented any further analysis using the arrival-time method. These two methods yielded comparable estimates to stream gage and flume estimates of streambed infiltration rate determined later in the year, which were 2.4×10^{-5} and $1.2 \times 10^{-5} \text{ m s}^{-1}$, respectively (Lewis, 2000). Expressed as daily values for comparison with other studies in this work, the temperature-derived streambed percolation rate ranged from more than 2100 to 100 mm d^{-1} . These percolation rates represent initial, transient rates compared with the steady percolation rates estimated for the two other New Mexico sites. Also, the lack of perturbation of

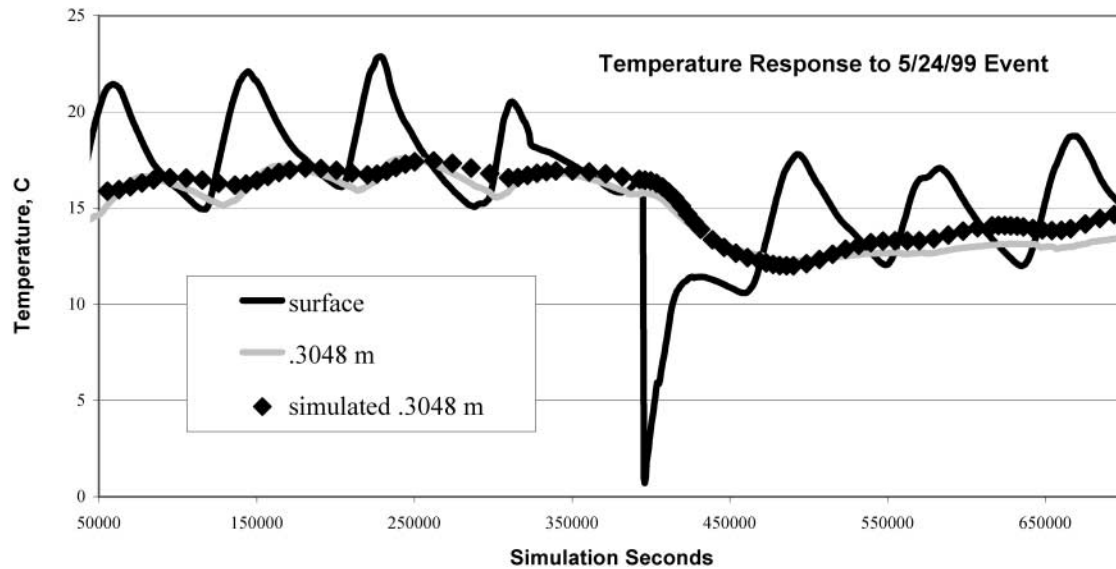


Fig. 6. The best-fit match of simulated streambed sediment temperatures at 0.3 m beneath the channel to observed temperatures for the May 1999 streamflow event on the Santa Fe River, NM.

the thermographs below 0.5 m, as compared with Bear Canyon thermographs, for example, suggests that percolation rapidly declined below this depth for this event in the Santa Fe channel.

In summary, the use of temperature profiles to examine shallow percolation appears to indicate a reasonable trend in terms of relative percolation rates. The temperature-derived percolation rates to a depth of 15 m for the perennial flows of the Rio Grande averaged in the 40 mm d^{-1} range. Shallow percolation rates to a depth of 3 m beneath Bear Canyon averaged in the 800 mm d^{-1} range during winter streamflows. Shallow percolation rates that were estimated between the surface and 2 m for ephemeral flows of the Santa Fe River ranged as high as 2000 mm d^{-1} during brief flow events lasting only hours. These trends were supported by surface water-based estimates of percolation that followed a similar trend. As shown below, these focused percolation estimates are orders of magnitude greater than deeper diffuse percolation rates estimated from temperature profiles.

ANALYSIS OF DEEP TEMPERATURE PROFILES IN ARID BASINS

Percolation rates generally vary slowly in deep vadose zones, and analytical solutions to the heat transfer equations may be appropriate. Beneath the region of temperature variations depicted in Fig. 1 (upper), heat transport is principally governed by the geothermal flux, advection associated with migration of water, conductive diffusion of sensible and latent heat, and long-term climate changes. In the deep vadose zones found in many arid regions, water flux may be very small, and it is often difficult to discern either its direction or magnitude. Thermal analysis can provide an assessment that is far less dependent on soil hydraulic properties and potentially reduce the uncertainty in the assessment of water flux direction and magnitude. The use of thermal data

to quantify water flux direction and magnitude in deep vadose zones becomes less quantitative as the flux decreases; however, thermal analysis, when conducted along with soil hydraulic and tracer analysis, can be used as an independent check on these results and can add a significant level of confidence. The development of independent methods of estimating soil water flux, such as thermal analysis, in deep vadose zones is essential to improving our estimates of groundwater recharge (Scanlon et al., 1997). In this section, a brief review of thermal transport, with special emphasis on the geothermal gradient in deep vadose zones is discussed along with application to observations and limitations of the analysis.

In the deep vadose zone, the primary heat transport direction can be assumed to be vertical. In the saturated region where flow may be dominated by lateral flow, advective (transport by the flowing phase) or convective (transport driven by gradients in fluid density) heat transport may serve to significantly alter both the regional heat transport and the magnitude of the geothermal gradient in the vadose zone. The general approaches taken in this work follow the work of Lachenbruch and Sass (1977). Assuming that conduction, advection, and diffusive transport of latent heat by water vapor are the dominant processes of heat transport in deep vadose zones, the governing one-dimensional equation for heat transport (Sophocleous, 1979) is:

$$C_s \frac{\partial T}{\partial t} = \frac{\partial}{\partial z} \left(K_T \frac{\partial T}{\partial t} \right) + \left(D_1 \frac{\partial \psi}{\partial z} \right) - C_w q_1 \frac{\partial T}{\partial z}, \quad [7]$$

where C_s represents the volumetric heat capacity of the bulk medium ($\text{J m}^{-3} \text{ } ^\circ\text{C}^{-1}$); K_T is the thermal conductivity of the medium ($\text{W m}^{-1} \text{ } ^\circ\text{C}^{-1}$); and D_1 is the product of the latent heat of vaporization (J kg^{-1}), fluid density (kg m^{-3}), and vapor conductivity (m s^{-1}). Equation [7] is similar in form to Eq. [1], with the addition of diffusive transport of latent heat by vapor as represented by the second term on the right-hand side.

This equation can be used in an inverse approach to estimate q_1 through a deep vadose zone if vadose zone temperatures are known. If the fluid flux is uniform, q_1 can be considered equivalent to the percolation rate (downward) or the discharge rate (upward) through the vadose zone. Solution of Eq. [7] requires initial and boundary conditions, soil thermal properties, and rates of fluid flux to derive the temperature distribution in the vadose zone. Under conditions of large thermal gradients and significant water flow, Eq. [7] must be coupled with the governing equation for the fluid (e.g., Eq. [5]) to obtain the correct thermal and fluid distributions. However, often the distribution of temperatures with depth, either from buried sensors or borehole logs, is the only environmental parameter monitored, such that Eq. [7] may be a reasonable option to obtain estimates of downward, upward, or negligible water flux.

Equation [7] may be simplified by assuming steady-state conditions and that the primary heat transport mechanisms are conduction and advection of heat by the liquid water phase. This represents a significant simplification relative to the previous analysis for stream-channel infiltration, where transient boundary conditions dominate. Tyler et al. (1996) showed that nonisothermal vapor transport in deep vadose zones of southern Nevada may be in the range of 0.02 mm yr^{-1} . Considering the heat content of this amount of vapor, vapor phase latent heat transport would comprise $<3\%$ of 1 heat flow unit (where 1 heat flow unit is approximately equal to $4.2 \times 10^{-4} \text{ J s}^{-1} \text{ m}^{-2}$) and can probably be ignored when only considering heat flux. Even when the nonisothermal vapor flux is a significant component of the heat budget, it may only vary slightly with depth, provided the thermal gradient is relatively constant and the range of temperature in the vadose zone is small. As a result, the diffusive transport of latent heat can be considered, to first order, to be a constant throughout the deep vadose zone and should not alter the shape of the geothermal gradient, only its magnitude. Therefore, thermal methods can be applied to vadose zones dominated by vapor transport, though the vapor phase component cannot be predicted. However, as shown by Walvoord et al. (1999), vapor transport may have significant impacts on the distribution of water potential in deep vadose zones. Further, if we limit our analysis to regions of small temperature gradients (i.e., deep in the vadose zone where the coupling between water and heat transport is limited), this leads to a more simplified analysis.

Under these assumptions and the assumptions of homogeneity of thermal properties and temporal stability, Eq. [7] can be reduced (Lachenbruch and Sass, 1977; Bredehoeft and Papadopoulos, 1965) to the following energy balance for the vadose zone profile:

$$\frac{\partial}{\partial z} \left(K_T \frac{\partial T}{\partial z} - C_w q_1 T \right) = 0. \quad [8]$$

Representing the boundary conditions correctly for Eq. [8] requires some discussion. The upper boundary condition can often be considered to be the average annual air temperature. The lower boundary tempera-

ture at the water table is more problematic. If the water table is treated as a constant temperature boundary condition, the thermal regime is mathematically decoupled from that of the saturated zone. This limits the need for specific hydraulic details of the saturation zone, with the observed temperature at the water table reflecting the combined effects of steady heat transport in the saturated and unsaturated zones. Such an approach is identical to that of Bredehoeft and Papadopoulos (1965), who used the temperature distribution in an aquitard surrounded by aquifers of differing temperatures to estimate leakage through the aquitard. The aquifer temperatures were assumed to be unaffected by the transport of heat through the aquitard. Under conditions of no advective transport of heat in the vadose zone via fluid flux, such an assumption is valid. However, if the rate of water flux is large and hence the rate of advective transport to the water table is large, the groundwater temperatures can be altered by this transport. Sophocleous (1979) pointed out that the analysis of Bredehoeft and Papadopoulos (1965) may have limited application in the saturated zone because of thermally driven liquid flow in the aquitard that may significantly affect the thermal distribution and lead to erroneous results. However, for the deep vadose zones at low water contents considered in this work, thermally driven liquid flow is likely to be insignificant because of the small hydraulic conductivity values and small thermal gradients.

Frenchman Flat, Nevada

Frenchman Flat, Nevada is typical of a sediment-filled basin of the Basin and Range Province and is given as an example of the analytical approach. For this deep setting, it is reasonable to assume that the temperature of the bottom water table boundary is constant, and subsequently unaffected by advective heat transport by fluid flux in from the vadose zone. The assumption is valid if groundwater temperatures are primarily governed by factors other than q_1 and if its value is small. There are many processes that will affect the temperature at the water table, including many that are independent of the vadose zone, such as local volcanic activity or groundwater flow paths, and these factors must be included in a comprehensive analysis of vadose zone temperatures. The vadose zone thermal properties are assumed to be uniform with depth, although they certainly will vary as saturation is approached at the water table. These assumptions may be limiting in some cases and clearly point out the need for additional numerical studies.

Under the above assumptions Eq. [8] can be solved easily to yield the temperature distribution as a function of the fluid flux and vadose zone thermal properties (Bredehoeft and Papadopoulos, 1965):

$$\frac{T_0 - T(z)}{T_w - T_0} = \frac{1 - \exp(z/z^*)}{1 - \exp(L/z^*)}, \quad [9]$$

where T_0 represents the temperature at the land surface, T_w represents the temperature of groundwater, $z^* = K_T/$

$q_1 C_w$, L is the thickness of the vadose zone. For small values of q_1 , the temperature distribution increases linearly with depth; as q_1 increases, the temperature profile becomes progressively concave upward in a similar fashion to that shown in Fig. 1 (upper). A series of solutions with a range of fluid flux or groundwater recharge values can be matched to observed borehole data to determine the best fit.

Temperature data from deep basin-fill vadose zones are relatively limited. Sass et al. (1988) presented a series of vadose and saturated zone temperatures from Yucca Mountain in southern Nevada, and reported generally linear profiles of temperature in this fractured rock vadose zone, suggesting primarily conductive heat transfer. Reynolds Electrical and Engineering Co. (1994) reported vadose zone temperatures from three boreholes completed in Frenchman Flat, which is two basins to the south of Yucca Mountain. Thermocouples were placed at 30- to 60-m intervals in boreholes drilled with air to minimize drilling impact on temperature, then back-filled. The water table is stable at a depth of approximately 240 m at this site. The vadose zone consists primarily of alluvial sediments with low volumetric water contents (8–12%) and was extensively sampled (both chemically and hydraulically) to determine the rate of water flux through the vadose zone. Tyler et al. (1996) reported that based on soil water tracers from these three boreholes, recharge through the vadose zone last occurred at 20 000 and 120 000 yr before present.

Figure 7 shows the vadose zone temperature distribution as measured by thermocouples from PW-1, one of the three boreholes in Frenchman Flat approximately a year after drilling and installation. Temperatures linearly increase from 18.45°C at a depth of 30 m to 20.74°C at a depth of 215 m. The calculated geothermal gradient (0.012°C m⁻¹) is low and is consistent with the generally low heat fluxes observed in the southern Great Basin. The low heat fluxes are postulated to be the result of large-scale, lateral heat transfer in the confined carbonate aquifers at depth (Lachenbruch and Sass, 1977). In Fig. 7 the predicted vadose zone temperatures from Eq. [9] are plotted for downward flux conditions of 1, 10, and 50 mm yr⁻¹. An effective thermal conductivity of 0.8 J s⁻¹ m⁻¹ °C⁻¹ was assumed, which is representative of sand at water contents of approximately 8% by volume (Hillel, 1980; Sophocleous, 1979). The results are somewhat sensitive to the chosen value of effective thermal conductivity and point out the need to include laboratory testing of this parameter along with typical soil physical and hydraulic parameters. At recharge rates <10 mm yr⁻¹ for the thermal properties chosen, the temperature distribution is essentially linear with depth, indicating the dominance of conductive heat transport over heat transported by percolation of cooler water. At higher rates of recharge, the heat transfer is dominated by advection and the shallow vadose zone approaches isothermal conditions. At these higher rates of recharge, it is important to note that the groundwater temperature (the assumed lower constant temperature boundary condition) may be reduced by the recharging

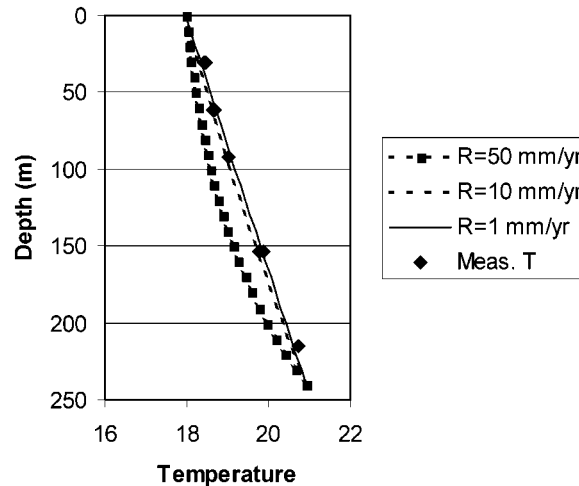


Fig. 7. Measured temperatures profile (solid diamonds) beneath Frenchman Flat, NV, compared with three analytical solutions with percolation rates of 1, 10, and 50 mm d⁻¹.

waters. At these higher rates of recharge, the choice of a constant lower boundary condition is not entirely correct. However, the linearity in the observed temperature profiles (with a less mean square coefficient, $R^2 = 0.986$) suggests that downward recharge rates are very small. Given the difficulty in resolving fluxes <10 mm yr⁻¹ with Eq. [9], the thermal data indicates very low downward or upward fluxes of <10 mm yr⁻¹. Previous work (Tyler et al., 1996) with chemical tracers suggested that downward migration was essentially zero. Water-potential data from the vadose zone show that hydraulic gradients are upward in the upper approximately 50 m, further reinforcing the concept of negligible recharge through this vadose zone. Recent work by Walvoord et al. (1999) and Phillips et al. (1999) further suggests that downward liquid flux in the vadose zone below 50 m may be balanced by upward vapor flux driven by the thermal gradient. In this case, thermal conduction is the dominant heat transport mechanism and serves to preserve the linear temperature gradient.

In summary, analysis of deep vadose zone temperatures using the simplifying assumption necessary for an analytical approach provides an independent method to aid in quantifying steady diffuse percolation and potential recharge. While the method has limited resolution at low fluxes, the thermal data are a vital, robust, and independent assessment, indicating that vadose fluxes are exceedingly low within the deep basin sediments underlying Frenchman Flat.

ANALYSIS OF DEEP TEMPERATURE PROFILES UNDERLYING ARID MOUNTAINOUS TERRAIN

The third case study requires a full description of two-phase heat and groundwater transport because of the complex stratigraphy of the fractured bedrock typical beneath mountainous terrain in arid environments. For most deep vadose zone profiles, it is reasonable to assume steady-state conditions, and a heat-balance equation in a partially saturated porous or fractured media

can be derived by considering heat-transport processes into and out of a control volume, much as the heat balance would be calculated for a computation cell in a finite difference model as expressed below:

$$\begin{aligned} \left(-K_T \frac{\delta T}{\delta z}\right)_2 &= \left(-K_T \frac{\delta T}{\delta z}\right)_1 - q_{l,m} c_l \Delta T \\ &\quad - q_g (c_g \Delta T - H_v (\chi_{v2} - \chi_{v1})) \\ &\quad - H_v \left[\left(-D_v \frac{\delta \rho_v}{\delta z}\right)_2 - \left(-D_v \frac{\delta \rho_v}{\delta z}\right)_1 \right], \end{aligned} \quad [10]$$

where c_l is the specific heat of the liquid water ($4.187 \times 10^3 \text{ J kg}^{-1} \text{ }^\circ\text{C}^{-1}$), ΔT is the temperature difference between elevations z_2 and z_1 ($^\circ\text{C}$), $q_{l,m}$ and q_g are the liquid and gas mass fluxes ($\text{kg s}^{-1} \text{ m}^{-2}$), c_g is the specific heat of the bulk gas ($1.1 \times 10^3 \text{ J kg}^{-1} \text{ }^\circ\text{C}^{-1}$), H_v is the heat of vaporization ($2.45 \times 10^6 \text{ J kg}^{-1}$); χ_{v2} and χ_{v1} are the vapor mass fractions of the gas at elevations z_2 and z_1 (kg kg^{-1}), D_v is the effective water vapor diffusivity in air ($\text{m}^2 \text{ s}^{-1}$), and ρ_v is the density of vapor (kg m^{-3}). The term on the left side of the equation is the conductive heat flux at elevation z_2 , which can be thought of as a function of the conductive heat flux at a lower elevation z_1 and the changes in the conductive heat flux resulting from the processes of liquid percolation, advective transport of sensible and latent heat in the gas phase, and diffusive transport of latent heat by water vapor. If the heat transport terms associated with gas and vapor transport are small relative to the percolation flux term, the liquid flux can be calculated directly from the temperature profile by considering the difference in the conductive heat flux at elevations z_2 and z_1 (Rousseau et al., 1999, p. 189). However, because the heat of vaporization (H_v) is quite large compared with other constants in Eq. [10], evaporation of what might normally be considered a small amount of water can have a large effect on the conductive heat flux, so processes that include the H_v term require careful evaluation. The potential significance of evaporative heat consumption can be illustrated by equating heat consumed to maintain thermal equilibrium between the rock and downwardly percolating water with that consumed by evaporation:

$$q_l c_l \Delta T = q_v H_v \quad [11]$$

where q_v is the evaporation rate ($\text{kg s}^{-1} \text{ m}^{-2}$). As an example, an evaporation flux of only 0.17 mm yr^{-1} results in the same consumption of heat as water percolating at 10 mm yr^{-1} through an unsaturated zone with a 10°C temperature difference.

Using the Eq. [10] approach, borehole temperature estimates of water flux suggest several possible advantages and disadvantages over other flux estimation methods. First, measurements of thermal conductivity and subsurface temperature are easy to make compared with measurements of unsaturated hydraulic conductivity and water potential. Second, thermal conductivity is a relatively linear function of saturation, and therefore subject to less uncertainty than other saturation-dependent quantities, such as hydraulic conductivity, that vary logarithmically with saturation. Also, temperature pro-

files may provide a meaningful long-term average of flux because temperatures below the depths affected by the annual temperature change respond slowly to changes in percolation flux because of the large mass and heat capacity of the rock. Finally, if thermal equilibrium is achieved between the rock and water, temperature measurements made in the rock will reflect the mass rate of water movement in both the matrix and fractures. The most significant disadvantage of deep temperature-based estimates of flux is that other heat transport processes, including vapor diffusion, convective gas transport, barometric pumping (particularly along faults), and topographic effects, may be operating in conjunction with advective liquid flux. Neglecting the effects of these processes without justification may significantly affect temperature-based estimates of flux. Data from beneath Yucca Mountain, Nevada provide an excellent case study of the advantages and limitations of this approach.

Yucca Mountain, Nevada

Mountainous terrain introduces complexities involving topography and air circulation not found when analyzing deep borehole temperature profiles in alluvial basin fill. Topographic effects result from the irregular nature of the surface boundary, which in itself results in a convergence or divergence of heat flow, and from microclimatic variations in ground-surface temperature related to slope aspect (Blackwell et al., 1980). Air circulation induced by topography (Weeks, 1987) increases the potential that the gas-phase transport of heat becomes a nonnegligible component of the overall heat balance.

Beneath Yucca Mountain the vadose zone consists of alternating layers of fractured, welded tuffs and relatively unfractured nonwelded tuffs (Scott et al., 1983). The welded tuffs have higher fracture permeabilities but lower intrinsic permeabilities than the nonwelded vitric tuffs (Montazer and Wilson, 1984; Flint, 1998). The thermal conductivities of the welded tuffs are about $2.0 \text{ J s}^{-1} \text{ m}^{-1} \text{ }^\circ\text{C}^{-1}$, or about twice those of the nonwelded tuffs (Sass et al., 1988). The generalized stratigraphy is shown for two boreholes in Fig. 8a and 8b, and the representative properties for different rock types and for the fracture network are given in Table 1.

Temperature and vapor pressure gradients result in the upward diffusion of water vapor in the deep welded tuffs below the PTn. To compensate for the vapor moving upward by diffusion, water deeper in the Topopah Spring Tuff must evaporate to maintain local equilibrium in vapor pressure. This process results in the upward transfer of latent heat and a possible reduction in the temperature gradient that could be erroneously attributed to water percolation. To estimate the magnitude of this effect, a calculation of the diffusive vapor flux was made using equations given in Cass et al. (1984), combined with typical temperature gradients of about $0.017^\circ\text{C m}^{-1}$ in the Topopah Spring Tuff (Sass et al., 1988). The upward diffusive vapor flux of 0.005 mm yr^{-1} estimated with these equations results in a latent

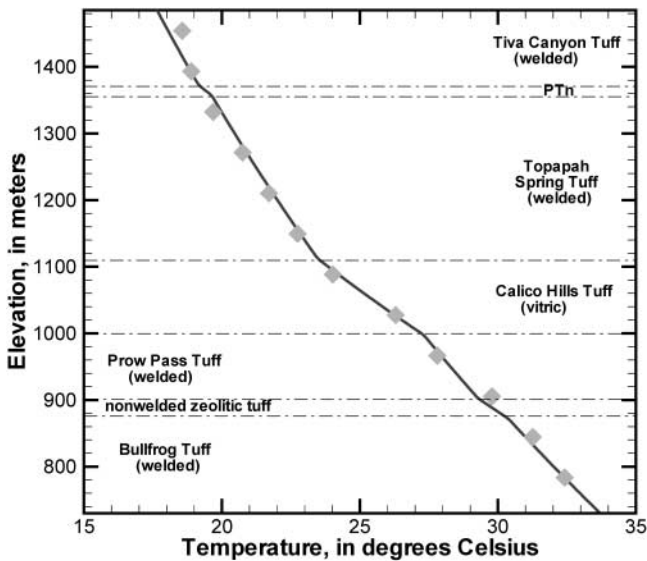


Fig. 8a. The observed rock-temperature profile for Borehole H-3 underlying Yucca Mountain, NV, compared with Case 1 simulation results, with stratigraphy shown in the body of the plot.

heat flux of about $4 \times 10^{-4} \text{ J s}^{-1} \text{ m}^{-2}$, or about two orders of magnitude less than the total conductive heat flux for much of Yucca Mountain. Therefore, in the absence of convective flow, the transport of latent heat by diffusion alone appears to be negligible in the overall heat balance.

Subsurface convective gas flow at Yucca Mountain is thought to be the result of gas-density differences caused by differences in air temperature and relative humidity inside and outside of Yucca Mountain (Weeks, 1987). Gas chemistry data and borehole gas-flow measurements indicate rapid convection of gas takes place in the shallow welded tuffs above the PTn, but that convective gas flow is slow or absent below the PTn (Thorsten et al., 1998; Yang et al., 1996). Therefore, although temperature data above the PTn may have been affected by gas flow, temperature data below and within the PTn have probably not been significantly affected by gas-flow processes.

The divergence of heat flux beneath ridges and convergence of heat flux toward washes also is a factor affecting borehole temperature profiles in rugged terrain (Blackwell et al., 1980; Rousseau et al., 1999). Unpublished two-dimensional heat transport simulations across Yucca Crest indicate these effects become less pronounced with depth, in part because the low thermal conductivity PTn obscures the effects of the surface

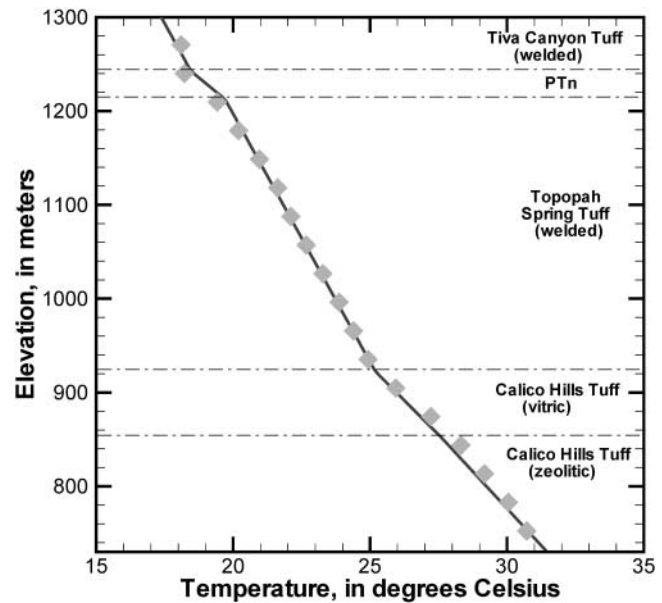


Fig. 8b. The observed rock-temperature profiles for Borehole WT-2 underlying Yucca Mountain, NV, compared with Case 1 simulation results, with stratigraphy shown in the body of the plot.

topography on temperatures in the deeper rocks. Therefore, although the one-dimensional numerical simulations presented below cannot account for the effects of topography on heat flow, most of the data used in the percolation estimates originates from depths relatively unaffected by these processes.

Borehole temperature data have been used to estimate percolation flux at Yucca Mountain using both numerical models (Rousseau et al., 1999; Flint et al., 2002; Bodvarsson et al., 2002) and analytical solutions (Bodvarsson et al., 1997). In these analyses, percolation rate was considered to be the only uncertain parameter in the models, and although the sensitivity of the modeled borehole temperatures to percolation rate was examined, no attempts were made to quantify the effects of other uncertain variables. However, there is also some uncertainty in the ground-surface temperatures that are used as the upper boundary condition and in the thermal conductivity values used in the models because of gas-flow processes, seasonal effects in the shallow rocks (Fig. 1) not reflected in the one-time temperature measurements, and microclimatic effects (Blackwell et al., 1980). To investigate the effects of uncertainty in ground-surface temperatures and thermal conductivity on estimates of percolation rate, the numerical model

Table 1. Summary of rock properties used in the simulations. S_{wr} , α , and β refer to parameters of the van Genuchten (1980) relative permeability and moisture retention functions. Matrix hydrologic properties are from Flint (1998). Thermal conductivities are based on data in Sass et al. (1988).

Rock unit	Permeability m^2	Porosity	Thermal conductivity $\text{W m}^{-1} \text{ } ^\circ\text{C}^{-1}$	S_{wr}	α m^{-1}	β
Welded tuff	4.1×10^{-18}	0.11	2.00	0.18	6.3×10^{-3}	1.470
PTn	9.0×10^{-14}	0.50	0.90	0.10	0.3345	1.427
Calico Hills (vitric)	5.6×10^{-14}	0.34	1.10	0.060	0.9608	1.294
Calico Hills (zeolitic)	4.6×10^{-18}	0.33	1.20	0.200	0.0386	1.290
Fracture continuum†	2.5×10^{-10}	0.01	—	0.01	4.000	2.917

† The fracture continuum was assumed to exist in all hydrologic units and was combined with the matrix continuum to form a composite porosity media as described in Zyvoloski et al. (1997).

Table 2. Results of FEHM/PEST simulations.†

Variable	Case no.	Borehole WT-2			Borehole H-3		
		Estimate	Lower 95% CI	Upper 95% CI	Estimate	Lower 95% CI	Upper 95% CI
T	1	17.4	17.01	17.74	17.65	17.23	18.08
T	2	17.14	16.73	17.56	17.65	17.18	18.14
T	3	17.15	16.7	17.61	17.65	17.31	17.99
Flux	1	0.20‡	-3.5¶	3.9	11.2	7.8	14.5
Flux	2	0.02‡	-7.8¶	7.8	11.0	3.3	18.7
Flux	3	0.2‡	-3.4¶	7.2	9.3	5.4	13.3
K_{welded}	1	2.00§	-	-	2.00§	-	-
K_{welded}	2	1.80	1.36	2.38	1.97	1.24	3.15
K_{welded}	3	1.79	1.40	2.28	1.79	1.40	2.28

† T is ground-surface temperature ($^{\circ}\text{C}$), flux is in millimeters per year, K_{welded} is the thermal conductivity of the welded unit ($\text{J s}^{-1} \text{m}^{-1}$), and CI is confidence interval.

‡ Value is at lower permissible bound.

§ Value is fixed in simulation.

¶ Negative percolation flux values indicate net evaporation from the borehole.

FEHM (Zyvoloski et al., 1997) was coupled with the parameter estimation code PEST (Doherty et al., 1994). PEST provides measures of the uncertainty of the estimates in the form of 95% confidence limits that reflect the combined uncertainty in all estimated parameters and the effects of any correlations that exist between the estimated parameters. Although these are linear confidence limits (i.e., they only reflect the uncertainty near the estimated values) and these confidence limits could change as the estimated values change, these confidence limits provide some indication of the reliability of the estimates. Models were created with the FEHM and PEST codes at two of the 25 or so Yucca Mountain boreholes at which temperature data are available (Sass et al., 1988; Rousseau et al., 1999). The temperature profiles at these two boreholes, WT-2 and H-3, previously were used to estimate recharge rates (Flint et al., 2002). Borehole WT-2 is located in a short, east-trending wash in central Yucca Mountain, and Borehole H-3 is located on Yucca Crest. The models extended from the ground surface to the water table, with a constant vertical grid spacing of 5 m. Although more than 30 separate hydrogeologic units have been identified in the vadose zone at Yucca Mountain (Flint, 1998), the models presented here used a simplified stratigraphy that includes five units, with the properties given in Table 1. Information on the depths of the stratigraphic intervals, major welding changes, and zones of zeolite development were taken from unpublished lithologic logs compiled by the U.S. Geological Survey (R. Spengler, personal communication, 1997) and from geophysical logs (Nelson, 1994, 1996). The simulations assumed a passive gas phase.

Three simulation cases were completed sequentially. For Case 1, percolation and ground-surface temperature at each individual borehole were determined using data only from that borehole. For Case 2, percolation, ground-surface temperature, and thermal conductivity of the welded tuffs (k_{welded}) at each borehole were determined, using data only from that borehole. For Case 3, percolation, ground-surface temperature, and thermal conductivity of the welded tuffs were determined jointly at both boreholes. In Case 3, flux and ground-surface temperature were allowed to differ between boreholes, but the thermal conductivities of the welded tuffs at both

boreholes were assumed to be the same. The estimated values and associated 95% confidence limits are given in Table 2. The measured temperature data and Case 1 simulation results are shown in Fig. 8a and 8b. The results indicate that although the estimated values of ground-surface temperature and percolation flux do not change much when k_{welded} is also estimated, the uncertainty in the flux and ground-surface temperature increases for Case 2 compared with Case 1, where k_{welded} is assumed to be known. When temperature data from both boreholes are used to estimate k_{welded} for Case 3, the uncertainty in each of the estimated parameters decreases compared with Case 2. Thus, if it can be assumed that thermal conductivity is relatively constant for a site, the simultaneous inversion of temperature profiles from multiple boreholes can reduce uncertainty in the percolation flux estimates at individual boreholes when the thermal conductivity and ground-surface temperature are also treated as uncertain parameters.

Fluxes of 11 and 0.2 mm yr^{-1} at Boreholes H-3 and WT-2, respectively, are in good agreement with fluxes of 10 and 0.5 mm yr^{-1} estimated at these boreholes using a more detailed stratigraphy and a trial-and-error calibration approach (Flint et al., 2002). Based on these comparisons, analysis of temperature profiles indicates that percolation in the range of 10 mm yr^{-1} may be representative near Borehole WT-2, while no significant flux appears to be present near Borehole H-2. In Table 2, results from the FEHM/PEST analysis provide constraints to flux, such that temperature-based flux estimates greatly limit the range of possible fluxes present in the deep vadose zone compared with the observed 170 mm yr^{-1} of annual precipitation incident at the top of the vadose zone.

CONCLUSIONS

Analysis of temperature profiles provides a promising tool for estimating percolation patterns for all three vadose environments examined in this work. Comparisons of shallow temperature profiles beneath stream channels for the perennial, seasonal, and ephemeral study reaches in New Mexico reveal a reasonable trend in terms of relative rates of focused percolation. Annual percolation rates beneath the perennial flows of the Rio

Grande averaged in the 40 mm d⁻¹ range. Seasonal percolation beneath Bear Canyon averaged in the 800 mm d⁻¹ range during winter streamflows. Transient percolation rates beneath the Santa Fe River ranged as high as 2000 mm d⁻¹ during brief flow events lasting only hours. These trends were supported by surface water-based estimates of streambed losses that followed a similar trend in magnitude when comparing the three sites.

A completely different flux pattern emerged from analysis of deep temperature profiles in southern Nevada. The temperature-derived diffuse percolation rates were estimated to be near zero in the deep basin sediments beneath Frenchman Flat and ranged from near zero to approximately 10 mm yr⁻¹ deep beneath Yucca Mountain. Temperature profiles exhibited a robust, increasingly concave patterns as percolation rates reached 10 mm yr⁻¹, in agreement with profiles predicted by both the analytical solution and the complex simulation model. Though the resulting magnitudes represent a negligible flux relative to the magnitudes estimated for focused percolation beneath New Mexico stream channels, the observed temporal stability of deep vadose zone temperature profiles indicates steady, long-term fluxes with potentially wide aerial extent.

ACKNOWLEDGMENTS

The authors would like to thank Jim Bartolino, USGS, for the Rio Grande Data; Amy Lewis, Sangre de Cristo Water, Santa Fe, NM, for surface water data for the Santa Fe River; Amy Stewart, Philip Williams and Associates, San Francisco, CA, for analysis of the Santa Fe River data; and Rich Niswonger, U.C. Davis and USGS, for analysis of the Bear Canyon data. The authors would also like to thank Joe Rousseau, USGS, and Paul "Ty" Ferre, University of Arizona, for thoughtful reviews. Efforts of the second author were funded in part by National Science Foundation Grant EAR-9614646.

REFERENCES

- Bartolino, J.R., and R. Niswonger. 1999. Numerical simulations of vertical ground-water fluxes of the Rio Grande from ground-water temperature profiles, Central New Mexico. *Water Resour. Invest. Rep.* 99-42-12. U.S. Geological Survey, Reston, VA.
- Blackwell, D.D., J.L. Steele, and C.A. Brott. 1980. The terrain effect on terrestrial heat flow. *J. Geophys.* 85:4757-4772.
- Bodvarsson, G.S., E.M. Kwicklis, C. Shan, A. Ritcey, and Y.S. Wu. 2002. Estimation of percolation flux from temperature data. *J. Contam. Hydrol.* In press.
- Bodvarsson, G.S., C. Shan, A. Htay, A. Ritcey, and Y.S. Wu. 1997. Estimation of percolation fluxes from temperature data. In G.S. Bodvarsson et al. (ed.) *The site-scale unsaturated-zone model of Yucca Mountain, Nevada, for the Viability Assessment*, Chapter 11. Yucca Mountain Site Characterization Project Rep. LBNL-40376, UC-814. Lawrence Berkeley National Laboratory, Berkeley, CA.
- Bouyoucos, G. 1915. Effects of temperature on some of the most important physical process in soils. *Mich. Coll. Ag. Tech. Bull.* 24. Michigan State Univ., East Lansing, MI.
- Bredehoeft, J.D., and I.S. Papadopoulos. 1965. Rates of vertical ground-water movement estimated from earth's thermal profile. *Water Resour. Res.* 1:325-328.
- Buckingham, E. 1907. *Studies on the movement of soil moisture.* USDA Bureau of Soils Bull. 38. U.S. Gov. Print. Office, Washington, DC.
- Cartwright, K. 1974. Tracing shallow groundwater systems by soil temperature. *Water Resour. Res.* 10:847-855.
- Cass, A., G.S. Campbell, and T.L. Jones. 1984. Enhancement of thermal water vapor diffusion in soil. *Soil Sci. Soc. Am. Proc.* 48:25-32.
- Constantz, J., and C.L. Thomas. 1996. The use of streambed temperatures profiles to estimate depth, duration, and rate of percolation beneath arroyos. *Water Resour. Res.* 32:3597-3602.
- Constantz, J., and C.L. Thomas. 1997. Streambed temperature profiles as indicators of percolation characteristics beneath arroyos in the Middle Rio Grande Basin, USA. *Hydrol. Process.* 11:1621-1634.
- Constantz, J., C.L. Thomas, and G. Zellweger. 1994. Influence of diurnal variations in stream temperature on streamflow loss and groundwater recharge. *Water Resour. Res.* 30:3253-3264.
- de Vries, D.A. 1963. Thermal properties of soils. p. 210-235. In W.R. van Wijk (ed.) *Physics of the plant environment.* North-Holland, Amsterdam, The Netherlands.
- Doherty, J., L. Brebber, and P. Whyte. 1994. PEST: Model independent parameters estimation. *Watermark Computing*, Brisbane, Australia.
- Flint, A.L., L.E. Flint, E.M. Kwicklis, J.T. Fabryka-Martin, and B.S. Bodvarsson. 2002. Estimating recharge at Yucca Mountain, Nevada: Comparison of methods. *J. Hydrogeol.* 10:180-204.
- Flint, L.E. 1998. Characterization of hydrogeologic units using matrix properties, Yucca Mountain, Nevada. U.S. Geological Survey Water-Resources Investigations Rep. 97-4243. U.S. Geol. Surv., Reston, VA.
- Healy, R.W. 1990. Simulation of solute transport in variably saturated porous media with supplemental information on modification of the U.S. Geological Survey's computer program VS2D. U.S. Geol. Surv. Water Res. Invest. Rep. 90-4025. U.S. Geol. Surv., Reston, VA.
- Healy, R.W., and A.D. Ronan. 1996. Documentation of the computer program VS2DH for simulation of energy transport in variably saturated porous media-modification of the U.S. Geological Survey's Computer Program VS2DT. U.S. Geological Survey Water-Resources Investigation Rep. 96-4230. U.S. Geol. Surv., Reston, VA.
- Hillel, D. 1980. *Fundamentals of soil physics.* Academic Press, New York.
- Izbicki, J.A., and R.L. Michel. 2002. Use of temperature data to estimate infiltration from intermittent streams in the western Mojave Desert, USA. In *Recharge Processes*, Intern. Hydrol. Soc. Proceedings. [CD-ROM] Adelaide, Australia. Int. Assoc. of Hydrology, Palmerston, Australia.
- Kipp, K.L. 1987. HST3D: A computer code for simulation of heat and solute transport in three-dimensional ground-water systems. U.S. Geological Survey Water Resources Investigations Rep. 86-4095. U.S. Geol. Surv., Reston, VA.
- Lachenbruch, A.H., and J.H. Sass. 1977. Heat flow in the United States and thermal regime of the crust. p. 626-675. In J.G. Heacock (ed.) *The earth's crust: Its nature and physical properties.* Geophysical Monogr. 20. American Geophysical Union, Washington, DC.
- Lapham, W.W. 1989. Use of temperature profiles beneath streams to determine rates of vertical ground-water flow and vertical hydraulic conductivity. U.S. Geol. Surv. Water Supply Paper 2337. U.S. Geol. Surv., Reston, VA.
- Lewis, A.C. 2000. Seepage study for the Santa Fe River. Sangre de Cristo Water Div., Misc. Rep. Ser. City of Santa Fe, NM.
- Montazer, P., and W.E. Wilson. 1984. Conceptual hydrologic model of flow in the unsaturated zone, Yucca Mountain, Nevada. *Water Resources Investigations Rep.* 84-4355:55. U.S. Geol. Surv., Reston, VA.
- Nelson, P.H. 1994. Saturation levels and trends in the unsaturated zone, Yucca Mountain, Nevada. p. 2774-2781. *Proceedings of the Fifth Annual International Conference on High-Level Radioactive Waste Management.* Vol. 4. American Nuclear Society, La Grange Park, IL.
- Nelson, P.H. 1996. Computation of porosity and water content from geophysical logs, Yucca Mountain, Nevada. U.S. Geological Survey Open File Rep. 96-078. U.S. Geol. Surv., Reston, VA.
- Nightingale, H.I. 1975. Groundwater recharge rates from thermometry. *Ground Water* 18:340-344.
- Niswonger, R., and J.L. Rupp. 2000. Monte Carlo analysis of streambed seepage rates. p. 161-166. In *Riparian ecology and management in multi-land use watersheds.* Am. Water Resources Assoc., Portland, OR.
- Philip, J.R., and D.A. de Vries. 1957. Moisture movement in porous materials under temperature gradients. *Eos Trans. AGU* 38:222-232.

- Phillips, F.M., M.A. Plummer, and M.A. Walvoord. 1999. Chloride profiles in thick desert vadose zones: What do they really tell us? Abs. 51564. *In* Geological Society of America Program with Abstracts, A-88. GSA, Boulder, CO.
- Richards, L.A. 1931. Capillary conduction of liquids through porous mediums. *Physics* 1:318–333.
- Reiter, M. 2001. Using precision temperature logs to estimate horizontal and vertical groundwater flow components. *Water Resour. Res.* 37:663–674.
- Reynolds Electrical and Engineering Co. 1994. Site characterization and monitoring data from Area 5 pilot wells, Nevada Test Site, Nye County, Nevada. Contract Rep. DOE/NV/11432-74. Nev. Oper. Off., U.S. Dep. of Energy, Las Vegas, NV.
- Ronan, A.D., D.E. Prudic, C.E. Thodal, and J. Constantz. 1998. Field study and simulation of diurnal temperature effects on infiltration and variably saturated flow beneath an ephemeral stream. *Water Resour. Res.* 34:2197–2153.
- Rousseau, J.P., E.M. Kwicklis, and D.C. Gillies (ed.) 1999. Hydrogeology of the unsaturated zone, North Ramp Area of the Exploratory Studies Facility, Yucca Mountain, Nevada. U.S. Geological Survey Water-Resources Investigations Rep. 98-4050. U.S. Geol. Surv., Reston, VA.
- Sass, J.H., A.H. Lachenbruch, W.W. Dudley, Jr., S.S. Priest, and R.J. Munroe. 1988. Temperature, thermal conductivity, and heat flow near Yucca Mountain, Nevada: Some tectonic and hydrologic implications. U.S. Geological Survey Open File Rep. 87-649. U.S. Geol. Surv., Reston, VA.
- Scanlon, B.R. 1994. Water and heat fluxes in desert soils. 1: Field studies. *Water Resour. Res.* 30:709–719.
- Scanlon, B.R., and P.C.D. Milly. 1994. Water and heat fluxes in desert soils. 2: Numerical simulations. *Water Resour. Res.* 30:721–733.
- Scanlon, B.R., S.W. Tyler, and P.J. Wierenga. 1997. Hydrologic issues in arid, unsaturated systems and implications for contaminant transport. *Rev. Geophys.* 35:461–490.
- Scott, R.B., R.W. Spengler, S. Diehl, A.R. Lappin, and M.P. Chornack. 1983. Geologic character of tuffs in the unsaturated zone at Yucca Mountain, southern Nevada. p. 289–335. *In* J.W. Mercer et al. (ed.) Role of the unsaturated zone in radioactive and hazardous waste disposal. Ann Arbor Science, Ann Arbor, MI.
- Sophocleous, M. 1979. Analysis of water and heat flow in unsaturated-saturated porous media. *Water Resour. Res.* 15:1195–1206.
- Stallman, R.W. 1963. Methods of collecting and interpreting groundwater data. U.S. Geol. Surv. Water Supp. Paper 1544-H. U.S. Geol. Surv., Reston, VA.
- Stallman, R.W. 1965. Steady one-dimensional fluid flow in a semi-infinite porous medium with sinusoidal surface temperature. *J. Geophys. Res.* 70:2821–2827.
- Suzuki, S. 1960. Percolation measurements based on heat flow through soil with special reference to paddy fields. *J. Geophys. Res.* 65:2883–2885.
- Tabbagh, A., H. Bendjoudi, and Y. Benderitter. 1999. Determination of recharge in unsaturated soils using temperature monitoring. *Water Resour. Res.* 35:2439–2446.
- Taniguchi, M., and M.L. Sharma. 1990. Solute and heat transport experiments for estimating recharge. *J. Hydrol. (Amsterdam)* 119:57–69.
- Taniguchi, M., and M.L. Sharma. 1993. Determination of groundwater recharge using the change in soil temperature. *J. Hydrol. (Amsterdam)* 148:219–229.
- Thorntson, D.C., E. P. Weeks, H. Hass, E. Busenberg, L.N. Plummer, and C.A. Peters. 1998. Chemistry of unsaturated zone gases sampled in open boreholes at the crest of Yucca Mountain, Nevada: Data and basic concepts of chemical and physical processes in the mountain. *Water Resour. Res.* 34:1507–1529.
- Tyler, S.W., J.B. Chapman, S.H. Conrad, D.P. Hammermeister, D. Blout, J. Miller, and J.M. Ginanni. 1996. Soil water flux on the Nevada Test Site: Spatial and temporal variation over the last 120,000 years. *Water Resour. Res.* 32:1481–1499.
- Walvoord, M.A., F.M. Phillips, M.A. Plummer, and A. Wolfsberg. 1999. Thick desert vadose zones: What is the equilibrium state? Abs. 51036 *In* Geological Society of America Program with Abstracts, A-88. GSA, Boulder, CO.
- Van Duin, R.H.A. 1963. The influence of management on the temperature wave near the surface. Tech. Bull. 29. Wageningen Institute of Land and Water Manag., Wageningen, The Netherlands.
- Weeks, E.P. 1987. Effect of topography on gas flow in unsaturated fractured rock: Concepts and observations. p. 165–170. *In* D.D. Evans and T.J. Nicholson (ed.) Flow and transport through unsaturated, fracture rock. *Geophys. Monogr.* 42. Amer. Geophys. Union, Washington, DC.
- Yang, I.C., G.W. Rattray, and Y. Pei. 1996. Interpretation of chemical and isotopic data from boreholes in the unsaturated zone at Yucca Mountain, Nevada. U.S. Geological Survey Water-Resources Investigations Rep. 96-4058. U.S. Geol. Surv., Reston, VA.
- Zyvoloski, G.A., B.A. Robinson, Z.V. Dash, and L.L. Trease. 1997. User's manual for the FEHM application—A finite element heat- and mass-transfer code. Rep. LA-13306-M. Los Alamos National Laboratory, Los Alamos, NM.